COMMISSIONING AND INITIAL OPERATING EXPERIENCE WITH THE SNS 1 GEV LINAC*

Stuart Henderson, Spallation Neutron Source, Oak Ridge National Laboratory, Oak Ridge TN, USA

Abstract

The Spallation Neutron Source accelerator complex consists of a 2.5 MeV H⁻ front-end injector system, a 186 MeV normal-conducting linear accelerator, a 1 GeV superconducting linear accelerator, an accumulator ring and associated beam transport lines. The beam commissioning campaign of the SNS accelerator complex, initiated in 2002 and completed in May 2006, was performed in seven discrete runs as each successive portion of the accelerator was installed. The final beam commissioning run, in which beam was transported to the liquid mercury target was completed in May 2006. In the course of beam commissioning, most beam performance parameters and beam intensity goals have been achieved at low duty factor. The beam performance and beam dynamics measurements of the linac are described and the initial operating experience is summarized.

INTRODUCTION

The Spallation Neutron Source (SNS) is a short-pulse neutron scattering facility which was recently completed at Oak Ridge National Laboratory. The SNS construction project was a partnership of six US DOE national laboratories, each of which had responsibility for designing and manufacturing a portion of the facility. At 1.44 MW of proton beam power on target, the SNS will operate at beam powers a factor of 7 beyond that which has been previously achieved [1]. The SNS baseline parameters are summarized in Table 1.

Table 1: SNS Design Parameters

Beam Power on Target	1.44 MW
Beam Energy	1.0 GeV
Linac Beam Macropulse Duty Factor	6.0%
Beam Pulse Length	1.0 msec
Repetition Rate	60 Hz
Chopper Beam-On Duty Factor	68%
Peak macropulse H- current	38 mA
Average Linac H- current	1.6 mA
Ring accumulation time	1060 turns
Ring bunch intensity	1.6×10^{14}
Ring Space-Charge Tune Spread	0.15
Beam Pulse Length on Target	695 nsec

The SNS accelerator complex [2] consists of a 2.5 MeV H⁻ injector [3], a 1 GeV linear accelerator [4], an accumulator ring and associated beam transport lines [5]. The injector (also called the Front-End Systems) consists of an H- volume ion-source with 50 mA peak current capability [6], a Radio-Frequency Quadrupole and a

Medium Energy Beam Transport line for chopping and matching the 2.5 MeV beam to the linac. The linear accelerator consists of a Drift Tube Linac (DTL) with 87 MeV output energy, a Coupled-Cavity Linac (CCL) with 186 MeV output energy, and a Superconducting RF Linac (SCL) with 1 GeV output energy [7]. At full design capability the linac will produce a 1 msec long, 38 mA peak, chopped beam pulse at 60 Hz for accumulation in the ring.

The linac beam is transported via the High Energy Beam Transport (HEBT) line to the injection point in the accumulator ring where the 1 msec long pulse is compressed to less than 1 microsecond by charge-exchange multi-turn injection. According to design, beam is accumulated in the ring over 1060 turns reaching an intensity of 1.5×10^{14} protons per pulse. When accumulation is complete the extraction kicker fires during the 250 nsec gap to remove the accumulated beam in a single turn and direct it into the Ring to Target Beam Transport (RTBT) line, which takes the beam to a liquid-mercury target.

Staged commissioning of the accelerator complex, now complete, was performed in seven discrete beam commissioning runs (shown in Figure 1) which were devoted to commissioning the i) Front-End, ii) Drift Tube Linac Tank 1, iii) Drift Tube Linac Tanks 1-3, iv) Coupled Cavity Linac, v) Superconducting Linac, vi) High-Energy Beam Transport Line and Accumulator Ring, and vii) Ring to Target Beam Transport Line and the mercury target. Table 2 summarizes the main beam commissioning results, comparing beam measurements with design goals.

With the construction project complete, the SNS is now beginning initial low-power operation.
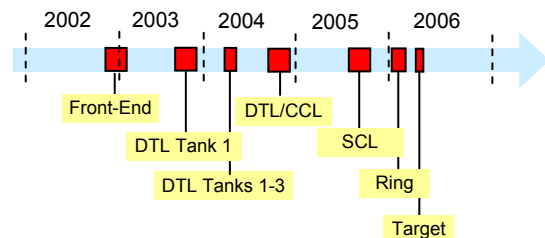
Figure 1: SNS Beam Commissioning Schedule

BEAM COMMISSIONING TOOLS

Beam Diagnostic Systems

An overview of SNS diagnostic systems is given in [8]. The front-end diagnostic systems are utilized to quantify the linac input beam parameters. Systems include an inline x-y emittance station, a mode-locked laser system for longitudinal profile measurements, beam position and

current monitors. The normal conducting linac includes energy degrader/faraday cups located after each DTL tank, beam loss monitors, beam position and current monitors, and bunch-shape monitors [9] for longitudinal profile measurements at the entrance to the CCL. The superconducting linac includes beam loss, position and current monitors as well as a laser-based transverse profile measurement system [10].

Table 2: Beam parameters achieved in commissioning and early operations

Parameter	Design	Measured
Linac Transverse Output Emittance [π mm-mrad (rms, norm)]	0.4	0.3 (H) 0.3 (V)
CCL1 Bunch Length [deg]	3	4
Linac Peak Current [mA]	38	>38
Linac Output Energy [MeV]	1000	952
Linac Average Current [mA]	1.6	1.05 (DTL1) 0.012 (SCL)
Linac H$^-$ ions/pulse	1.6×10^{14}	1.0×10^{14}
Linac pulse length/rep rate/duty factor [msec/Hz/%]	1.0/60/6.0	1.0/60/3.8 (DTL1) 0.85/0.2/.017 (SCL)
Ring intensity	1.5×10^{14}	1.0×10^{14} (unbunched)
Beam intensity on target	1.5×10^{14}	5.0×10^{13}

Application Programs

Central to the success of the rapid beam commissioning of the SNS accelerator complex was a set of applications programs which were tested and available on day one of each commissioning phase. The XAL programming infrastructure [11] provided a powerful framework for rapid development and deployment of application programs. Approximately 50 application programs have been developed for commissioning and operation of the SNS accelerator complex. The SNS commissioning strategies and tuneup algorithms, written within the XAL framework, are described in [12].

Many of the commissioning algorithms rely heavily on accurate real-time modelling of the accelerator. An online-model of the linac has been developed [11] which includes single-particle tracking through individual RF gaps [13] to obtain the beam centroid arrival phase. Beam sizes are determined using an envelope approach [14]. Transport line modelling is also contained within the linac model. The linac model has been successfully benchmarked to Trace-3D and PARMILA [15]. The Ring online model at present consists of a linear, first-order transport model ignoring space-charge. These models are adequate for most of the commissioning operations since low-intensity beams are used for initial tuneup. The ring model has been successfully benchmarked to MAD and TRANSPORT. When multi-particle simulations are required to compare to commissioning data, the PARMILA and IMPACT [16] codes are used for the linac

dynamics, and the ORBIT [17] code is used for accumulator ring and transport line dynamics.

NORMAL CONDUCTING LINAC TUNEUP AND PERFORMANCE

Early normal-conducting linac beam commissioning results have been reported previously [18]. Updated measurements are described herein and presented in another contribution in these proceedings [19].

Extensive diagnostic systems, described above, allow thorough characterization of the MEBT beam prior to injection into the linac. The measured MEBT transverse emittances are 0.29 and 0.26 π mm-mrad (rms, norm), in the horizontal and vertical planes respectively. The RMS longitudinal beam profile, measured with a mode-locked laser system, is 18 degrees, which agrees with expectations.

Coarse determination of RF phase and amplitude setpoints are obtained using energy degrader/faraday cup scans, as described in [20]. More accurate determination of RF setpoints relies on comparisons of measured beam arrival phase data with model predictions. In the normal-conducting linac, RF setpoints are determined using the phase-scan signature matching [21] and "Delta-T" [22] techniques. In the phase-scan signature matching technique the difference in beam arrival phase at two BPMs downstream of the DTL tank or CCL module in question is recorded as a function of tank or module phase for a few different RF field amplitudes. While the small amplitude motion is linear, phase scans are performed over a wide range in cavity phase to take advantage of the non-linearity of large amplitude motion. The input beam energy, tank or module RF amplitude and relative beam/RF input phase are determined with a model based fit to data obtained at two or more RF amplitudes. Figure 2 shows an example for CCL module 2, where the curves show measured data and the points show the model results after fitting, for two RF amplitudes differing by 1%. As is evident, this method can be quite sensitive to the RF amplitude, and provides setpoint accuracy to within 1% and 1 degree.
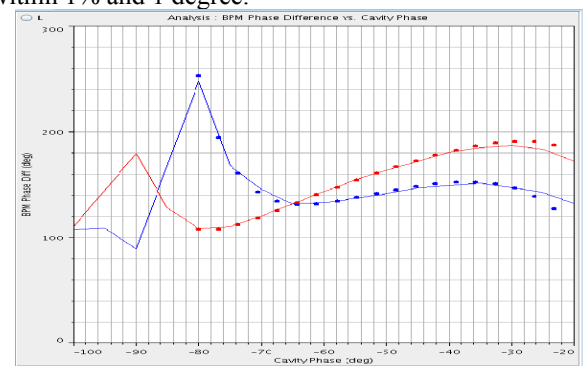
Figure 2: Results of phase-scan signature matching to determine RF setpoints. BPM phase difference is plotted vs. CCL module 2 phase. The curves show data for two RF amplitudes. The points show the results of model-based fitting.

Bunch lengths are measured at three locations in CCL module 1 with bunch shape monitors. The measured bunch length of 4 degrees is in good agreement with the model expectation of 3 degrees.

SUPERCONDUCTING LINAC TUNEUP AND PERFORMANCE

The superconducting linac consists of 81 independently powered cavities. The principal method in use for determining RF setpoints is the well-known time-of-flight based phase scan. In this method the difference in beam arrival phase between two downstream BPMs is recorded as the SCL RF cavity phase is scanned across the full 360 degrees. The resulting phase difference is very nearly sinusoidal and is readily fit to obtain the input energy, the cavity accelerating gradient and the relative beam-cavity phase [23]. The cavity phase is set according to the measured relative beam/cavity phase and the design synchronous phase (typically -20 degrees). Figure 3 shows a sample measurement in which the BPM phase difference is plotted vs. cavity phase. An analysis [23] shows that with a phase-scan stepsize of 5 degrees, one can achieve a setpoint accuracy of 1% in amplitude and 1 degree in phase. This method relies on the absolute phase measurement capability of the beam position monitor system which has been demonstrated [24].

Longitudinal tuneup of the superconducting linac proceeds by performing phase scans for each cavity sequentially along the linac (with all downstream cavities unpowered) and transporting the beam through several intermediate low-energy lattices appropriate for the output energy of the cavity in question. A typical SCL tuneup operation takes 16 hours.
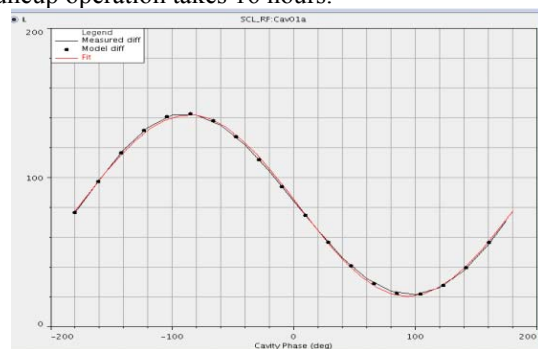
Figure 3: Downstream BPM phase difference vs. SCL cavity phase data (line) compared with results of model-based fitting (dots) and sinusoidal fitting (red).

In an effort to reduce tuneup time, other methods are being explored. A second method for determining cavity amplitudes and relative beam/RF phase utilizes the beam-induced signal generated by the beam drifting through an unpowered cavity [23]. In this technique, the phase and amplitude of the beam-induced cavity field is measured with the standard low-level RF control system. Agreement between this method and the time-of-flight method is within 1 degree in phase. This method is still under development and holds the promise of a more rapid RF setpoint determination.

TRANSVERSE DYNAMICS

Proper transverse matching is essential to minimize emittance and halo growth. Matching quadrupoles are available at the lattice transitions between MEBT and DTL, at the input to the CCL, between CCL and SCL, and between SCL and HEBT. Transverse matching is accomplished either by utilizing beam profile data to set matching quadrupoles, or by empirical adjustment of matching quadrupoles to minimize beam losses.

The most important linac beam quality measure is the transverse emittance growth. Sets of beam profile data from dual-plane wire scanner arrays in the CCL, SCL and HEBT allow measurement of the twiss parameters and transverse beam emittances. Gaussian fits to beam profile data were performed to obtain RMS beamsizes. Using a model-based fitting method and knowledge of the beam energy and quadrupole gradients, best-fit twiss parameters and RMS emittances were obtained. Table 3 shows a compilation of results performed during beam commissioning, showing that the emittance growth is consistent with the design specifications. It should be noted that the emittances are measured at beam currents varying from 20 mA to 38 mA, and that the typical measurement error is about 20%.

Table 3: Comparison of measured and expected RMS transverse beam emittances at four locations in the linac.

Location	Measured ε_x, ε_y π-mm-mrad (rms, norm)	Design ε_x, ε_y π-mm-mrad (rms, norm)
MEBT Entrance	0.22, 0.25	0.21
CCL Entrance	0.22, 0.25	0.33
SCL Entrance	0.27, 0.35	0.41
Linac Dump	0.26, 0.27	0.41
HEBT	0.50, 0.37	0.45

LINAC OPERATION

The linac has operated thus far with output beam energies in the range 550-950 MeV. In early low-power operations the linac output energy has been about 850 MeV. Linac beam current monitors for a typical beam pulse are shown in figure 4. This pulse has operating parameters as follows: 200 μs pulse length, 860 MeV, 18 mA peak current, 70% chopping duty factor, 12 mA average pulse current and 1.5×10^{13} H⁻ ions/pulse. The highest intensity beam pulse yet produced in the SNS linac is shown in figure 5. This pulse has parameters as follows: 880 μs pulse length, 930 MeV, 20 mA peak current, unchopped, and 1.0×10^{14} H⁻ ions/pulse. This single pulse intensity corresponds to that required for 1 MW operation, with a linac repetition rate of 60 Hz.
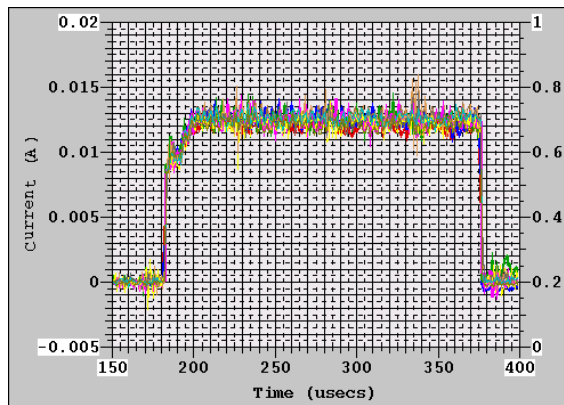
Figure 4: Overlay of 12 beam current monitors in the linac for a typical beam pulse.
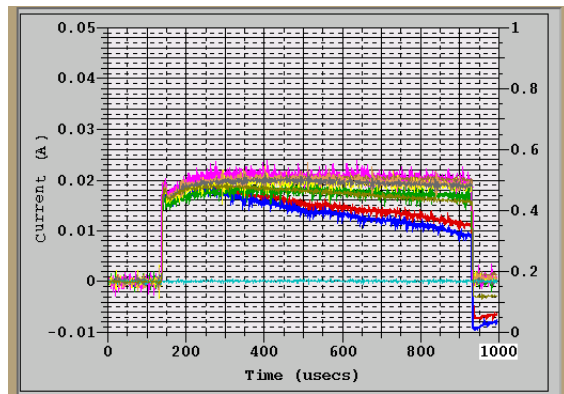
Figure 5: Overlay of 12 beam current monitors in the linac for a beam pulse of 1×10^{14} protons/pulse. The two lower current monitor traces have untuned droop correction.

One of the main benefits of a superconducting linac in a proton accelerator application is the operational flexibility that it affords. With individually powered cavities, downstream cavities can be adjusted in phase and amplitude to recover from a change in operating gradient of an upstream cavity. Thus, cavities which are offline may be readily "tuned around." This is in contrast to the situation in a normal conducting linac with long CCL modules, in which the design velocity profile is expressed in the module geometry itself; the loss of a module interrupts beam operation until a repair can be completed. Thus far in commissioning and initial operations we have taken advantage of that flexibility by operating with as many as 20 cavities unpowered in the initial tuneup, and now by operating routinely with 5 unpowered cavities. We anticipate that this flexibility will be important for achieving the high availability goals required by the user community.

To capitalize on that flexibility requires rapid fault recovery algorithms. A method for adjusting downstream cavity phases in response to an upstream cavity fault or setpoint change has been developed and successfully tested; preliminary results are described in [12, 25].

A snapshot of SCL cavity gradients is shown in figure 6. Two data points are plotted for each cavity: the lower point is the operating gradient during recent 840 MeV operation, and the upper point is the field limit. The difference indicates the operating margin.
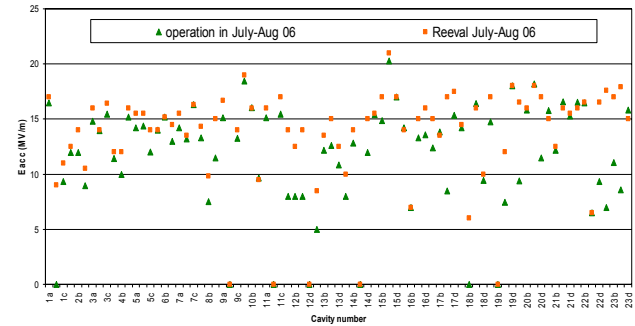
Figure 6: SCL cavity operating gradients (green) and gradient limits (orange).

Five cavities are unpowered at present: three due to out-of-range tuners, and two due to excessive fundamental power coupled through the HOM signal. About 10 cavities are operating at reduced gradients and/or repetition rates because they show abnormal fundamental frequency signals transmitted through the HOM couplers due mainly to electron-related activity [26]. In early operations, gradients were limited in some cavities by vacuum-related interlock trips. The signals from cold-cathode gauges installed near the fundamental power couplers were observed to extinguish. In some cases, the subsequent ignition of the emission current resulted in rapid bursts and oscillations of the output CCG current, unrelated to genuine vacuum activity, but nevertheless causing a trip in the interlock chain. After careful conditioning, proper operation of these CCG gauges was restored. Alternative vacuum interlock possibilities are being considered.

A typical beam loss distribution is shown in Figure 7. The data show beam losses for a single beam pulse of 255 μs length and 2×10^{13} H⁻ ions/pulse. At present low-power (2-5 kW) operation, losses just exceed the noise floor in the loss monitor readout system; peaks in the loss profile correspond to fractional losses of about 0.01% based on preliminary loss monitor response studies. Measured loss levels shown in figure 7, sustained in 2 kW running, lead to residual activation of less than 1 mRem/hr at 30 cm, which scales favourably to a few hundred kW of beam power. It should be emphasized that systematic transverse matching in the linac and HEBT has not yet been successfully demonstrated.
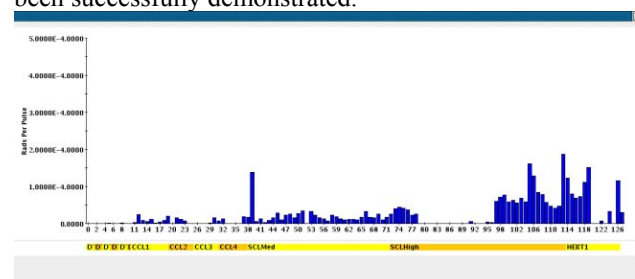
Figure 7: Typical linac beam loss profile.

Beam power is administratively limited at present to 10 kW. The beam power during one 24 hour period of neutron production is shown in figure 8. During this run the beam power was increased to 9.7 kW, sustained for four hours and then reduced to 2 kW.
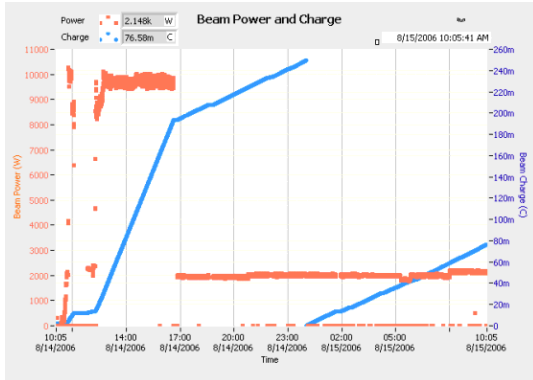
Figure 8: Beam power (red) and integrated protons on target (blue) during a 24 hour period of neutron production in August 2006. A beam power of 10 kW was achieved.

RF Amplitude and Phase Control

The SNS low-level RF system is described in [27]. In addition to feedback control of the cavity amplitude and phase, feedforward has proven essential for achieving the required amplitude and phase regulation in the presence of heavy beam loading. Typical amplitude and phase regulation errors are better than 1% and 1 degree respectively.

CONCLUSION

The commissioning of the SNS accelerator complex was completed in May 2006. The construction project was formally completed, on-time and within budget, in June 2006. Most beam quality and beam intensity goals were met or exceeded in commissioning. The SNS is now entering the initial low-power operations phase having delivered 10 kW of beam power on target. The two-year ramp up to 1 MW of beam power on target is beginning.

REFERENCES

[1] C. Prior et. al., Proc. PAC 2003, p. 1527
[2] N. Holtkamp, Proc. EPAC 2006.
[3] A. Aleksandrov, Proc. PAC 2003, p. 65
[4] D. Jeon, Proc. PAC 2003, p. 107
[5] J. Wei, Proc. PAC 2003, p.571
[6] R.F. Welton et. al., Proc. PAC 2005, p. 472; M. Stockli, these proceedings.
[7] I.E. Campisi, Proc. PAC 2005, p. 34
[8] S. Assadi, Proc. PAC 2003, p. 498.
[9] A. Feschenko et. al., Proc. LINAC 2004, p. 408.
[10] S. Assadi, these proceedings.
[11] J. Galambos et. al., Proc. PAC 2005 p. 79.
[12] J. Galambos, Proc. ICFA HB2006.
[13] B. Schnizer, Part. Acc. 2 (1971) 141.
[14] C.K. Allen et. al., Proc. PAC 2003, p. 3527.
[15] H. Takeda, LANL LA-UR-98-4478.
[16] J. Qiang et. al., J. Comp. Phys. 163 (2000) 434.
[17] J. Holmes et. al., ICFA Beam Dynamics Newsletter, Vol. 30, 2003.
[18] A. Aleksandrov, Proc. PAC 2005, p. 97
[19] A. Aleksandrov et. al., these proceedings.
[20] D. Jeon, these proceedings.
[21] J. Galambos et. al., Proc. PAC 2005, p. 1491.
[22] A. Feschenko et. al., Proc. PAC 2005, p. 3064.
[23] S. Henderson et. al., PAC 2005, p. 3423.
[24] C. Deibele et. al., these proceedings.
[25] J. Galambos et. al., these proceedings
[26] S. Kim et. al., these proceedings.
[27] H. Ma, et. al., these proceedings.